The Crop Journal 9 (2021) 794–804

Contents lists available at ScienceDirect

The Crop Journal

journal homepage: www.elsevier.com/locate/cj

Evaluation of maize root growth and genome-wide association studies of root traits in response to low nitrogen supply at seedling emergence

Xichao Sun [a,b], Wei Ren [a], Peng Wang [a], Fanjun Chen [a], Lixing Yuan [a], Qingchun Pan [a,*], Guohua Mi [a,*]

[a] College of Resources and Environmental Sciences, National Academy of Agriculture Green Development, Key Laboratory of Plant-Soil Interactions, Ministry of Education, China Agricultural University, Beijing 100193, China
[b] Agro-Environmental Protection Institute, Ministry of Agriculture and Rural Affairs, Tianjin 300191, China

ARTICLE INFO

Article history:
Received 9 December 2019
Revised 14 August 2020
Accepted 27 September 2020
Available online 28 November 2020

Keywords:
Genome-wide association study (GWAS)
Nitrogen
Maize
Root

ABSTRACT

Nitrogen (N) deficiency is one of the main factors limiting maize (*Zea mays* L.) productivity. Genetic improvement of root traits could improve nitrogen use efficiency. An association panel of 461 maize inbred lines was assayed for root growth at seedling emergence under high-nitrate (HN, 5 mmol L^{-1}) and low-nitrate (LN, 0.05 mmol L^{-1}) conditions. Twenty-one root traits and three shoot traits were measured. Under LN conditions, the root-to-shoot ratio, root dry weight, total root length, axial root length, and lateral root length on the primary root were all increased. Under LN conditions, the heritability of the plant traits ranged from 0.43 to 0.82, a range much wider than that of 0.27 to 0.55 observed under HN conditions. The panel was genotyped with 542,796 high-density single-nucleotide polymorphism (SNP) markers. Totally 328 significant SNP markers were identified using either mixed linear model (MLM) or general linear model analysis, with 34 detected by both methods. In the 100-kb intervals flanking these SNP markers, four candidate genes were identified. Under LN conditions, the protoporphyrinogen IX oxidase 2 gene was associated with total root surface area and the DELLA protein-encoding gene was associated with the length of the visible lateral root zone of the primary root. Under HN conditions, a histone deacetylase gene was associated with plant height. Under both LN and HN conditions, the gene encoding MA3 domain-containing protein was associated with the first whorl crown root number. The phenotypic and genetic information from this study may be exploited for genetic improvement of root traits aimed at increasing NUE in maize.

1. Introduction

Nitrogen (N) is one of the main factors limiting crop growth [1]. Over the past half century, global N use in agriculture has increased sevenfold [2,3]. However, only 30%–40% of applied N is utilized by most crops [4,5]. Overapplication of N fertilizers leads to water eutrophication [6,7], acid rain, soil acidification [8], increased greenhouse gas emissions [9], atmospheric N deposition [10], and other severe environmental problems. Maize (*Zea mays* L.) is the world's largest food crop, and global maize production accounts for about one-fifth of the total N fertilizers used in agricultural production [11]. Thus, increasing N efficiency in maize is crucial for ensuring food security and environmental sustainability [12].

Root architecture plays an important role in plant nutrient and water acquisition. Maize genotypes with optimal root system architecture are more efficient in N acquisition from the soil [13–17]. Under acute conditions of insufficient N supply, axial root and lateral root growth are increased [18–20]. However, long-term chronic N deficiency may inhibit lateral root growth [21,22]. Larger root systems help the plant explore a larger soil volume to increase total N uptake [23]. Breeding new cultivars with N-efficient root system architectures would increase N use efficiency (NUE) in maize [14,24–26].

Root architecture is composed of complex quantitative traits with large natural variations. Owing to the complexity of root systems and the difficulty of identifying root phenotypes on a large scale, knowledge of the genetics of root architecture lags behind that in shoots. This situation has created a gap in our ability to genetically improve root traits [27]. Most root studies have focused on identifying quantitative trait loci (QTL) influencing root growth. Hund et al. [28] classified 161 root QTL into 24 QTL clusters by

* Corresponding authors.
E-mail addresses: panqingchun@cau.edu.cn (Q. Pan), miguohua@cau.edu.cn (G. Mi).

https://doi.org/10.1016/j.cj.2020.09.011

summarizing 15 mapping studies in nine genetic populations. Among these root QTL, Bins 1.07, 2.04, 2.08, 3.06, 6.05, and 7.04 were hotspots. Guo et al. [29] conducted a meta-analysis of 428 QTL associated with 23 maize root traits from 20 published papers and identified 53 meta-QTL and 45 possible candidate genes. Additional studies [30–32] also indicate that QTL for maize root traits and NUE are co-localized across multiple chromosomal regions.

Genome-wide association studies (GWAS) provide new opportunities for map-based cloning of root-trait genes [33]. In contrast to QTL or bi-parental linkage mapping, association mapping is based on existing populations. With improved methods to accurately position GWAS peaks, the time required to identify a single gene can be greatly reduced [34]. Using 384 maize inbred lines in a GWAS, Pace et al. [35] obtained 268 SNPs significantly associated with 22 seedling root traits, many of them located within 1 kb of gene models. Zaidi et al. [36] grew 396 tropical maize lines under drought and well-watered conditions and identified respectively 50 and 67 SNPs significantly associated with root functional and structural traits. Morosini et al. [37] used 64 tropical maize inbred lines to analyze maize tolerance under low N in the field and identified seven significant SNPs for low N tolerance index and total root length. The predicted candidate genes were involved mostly in transcriptional regulation and enzyme activity in the N cycle. Sanchez et al. [38] used 300 doubled-haploid exotic introgression lines to map 17 SNPs associated with root growth. T SNP S5_152926936 on chromosome 5 was found within the gene model *GRMZM2G021110*, which encodes a putative xaa-Pro dipeptidase that is expressed in seedling roots. To date, there have been no reports of GWAS and candidate-gene mining for maize root traits under low-N stress.

To elucidate the genetic basis of maize root growth and the response to low N supply at seedling emergence, we planted a panel of maize inbred lines under high- and low-N conditions. Our objectives were: (1) to characterize genetic variation in root phenotypic response to low N supply and (2) to identify, using GWAS, SNPs and candidate genes associated with root response to low-N stress.

2. Materials and methods

2.1. Plant materials

A panel of 508 maize inbred lines was used (Table S1). Because 47 of these failed to germinate and could not be used for further study, 461 lines were used. The maize panel includes three clear subpopulations: 31 stiff stalk (SS) lines, 121 non-stiff stalk (NSS) lines and 205 tropical/subtropical (TST) lines. The remaining 104 lines were classified as a mixed subpopulation, as they had membership probabilities <0.60 in any of the other subpopulations. The population captured wide geographic distribution and genetic diversity (Table S1; http://maizego.org/Resources.html). The panel has been described previously [39].

2.2. Experimental design

The panel of 461 maize inbred lines was grown in paper rolls in a greenhouse with a light/dark cycle of 13/11 h and a temperature of 18–36 °C. Two independent experiments with the same experimental design were conducted in September 2017 and September 2018. For each experiment, 80 seeds of each line were surface-sterilized in 10% (v/v) H_2O_2 for 40 min, washed 3 times with deionized water, and then soaked in saturated $CaSO_4$ solution for approximately 8 h. Seeds were then placed between sheets of filter paper soaked in deionized water and germinated in the dark at room temperature. When the roots were approximately 2 cm long (after about 1 day), four uniform seedlings were placed approximately 2 cm below the top edge of the filter paper and covered with another piece of wet filter paper, and both were rolled up. Three rolls, each containing plants of one maize inbred line, were placed upright in a 1-liter black plastic bucket filled with nutrient solution. The two different nutrient solutions were low N (LN, 0.05 mmol L^{-1}N) and high N (HN, 5 mmol L^{-1}N). The HN solution consisted of 2.5 mmol L^{-1} $Ca(NO_3)_2$, 0.75 mmol L^{-1} K_2SO_4, 0.25 mmol L^{-1} KH_2PO_4, 0.1 mmol L^{-1} KCl, 0.65 mmol L^{-1} $MgSO_4$, 0.13 mmol L^{-1} EDTA-Fe, 1.0 μmol L^{-1} $ZnSO_4$, 1.0 μmol L^{-1} H_3BO_3, 1.0 μmol L^{-1} $MnSO_4$, 0.1 μmol L^{-1} $CuSO_4$, and 0.005 μmol L^{-1} $(NH_4)_6Mo_7O_{24}$. The LN nutrient solution contained one hundredth of the N concentration [0.025 mmol L^{-1} of $Ca(NO_3)_2$], and the Ca^{2+} concentration was adjusted with $CaCl_2$ to the same level as that of HN. The other nutrient concentrations were the same as for HN. The pH of each solution was adjusted to 6.0 with KOH and HCl. Before being exposed to light, all the seedlings in about 1000 buckets were cultivated in the dark for 2 days until the cotyledons were approximately 2 cm long. Buckets were arranged in a completely randomized design.

2.3. Root and shoot phenotype measurement

After six days of growth in the N solutions, seedlings with three leaves were removed from the buckets for root and shoot measurements. Three paper rolls were selected as experimental replicates for each inbred line. Three healthy seedlings of the four in each paper roll were sampled and, for each trait, the mean of the three plants was taken as a replicate. Plants were divided into shoots and roots by cutting at the position where the first whorl crown roots occur on the stem, and the seeds were removed from the roots. Twenty-four seedling phenotypic traits were evaluated at two N levels. Shoot traits included shoot dry weight (SDW), plant height (PH) and chlorophyll content (SPAD) of the first leaf. Root traits included root-to-shoot ratio (RSR), root dry weight (RDW), total root length (TRL), total root surface area (TRSA), total root volume (TRV), total primary root length (TPRL), total primary root surface area (TPRSA), total primary root volume (TPRV), primary root length (PRL), length of the primary root apical unbranched zone (LAUZPR), length of the visible lateral root zone (LVLRZ), primary lateral root length (PLRL), visible lateral root number of the primary root (VLRNPR), average lateral root length of the primary root (ALRLPR), visible lateral root density of the primary root (VLRDPR), seminal root number (SRN), seminal root length (SRL), first-whorl crown root number (FWCRN), first-whorl crown root length (FWCRL), average root diameter (ARD) and average primary root diameter (APRD) (Table 1). Plant height was measured using a ruler, and the SPAD value was measured using a SPAD-502 chlorophyll analyzer (Minolta Camera Co. Ltd., Osaka, Japan). Shoots were then dried at 65 °C in an oven for 3 days, and shoot dry weight was recorded. Roots were placed into plastic ziplock bags and stored at −20 °C until they were measured. The primary root length, seminal root length, first whorl crown root length [40] and length of the primary root apical unbranched zone were measured with a ruler. The seminal roots and first whorl crown roots were manually counted. The root samples were then floated in water in a transparent plastic tray and scanned with a scanner. The traits TRL, TRSA, TRV, TPRL, TPRSA, TPRV, VLRNPR, ARD, and APRD were scanned and analyzed using the WinRHIZO 2004b software (Regent Instruments, Canada). Roots were then dried and weighed to determine root-to-shoot ratio. The traits are described in Table 1.

2.4. Statistical analysis

Best linear unbiased prediction (BLUP) for each trait was calculated using "lme4" in the R software as follows: lme4 = phenotype~

Table 1
Maize seedling trait measurements and descriptions.

Trait name	Abbreviations	Trait measurements and descriptions
Shoot-related traits		
Shoot dry weight (g plant^{-1})	SDW	Dried and weighed on a balance (0.0001 g)
Plant height (cm)	PH	Measured with a ruler
SPAD value of the first leaf	SPAD	Measured with a chlorophyll meter
Root traits		
Root-to-shoot ratio	RSR	Root dry weight/shoot dry weight
Root dry weight (g plant^{-1})	RDW	Dried and weighed on a balance (0.0001 g)
Total root length (cm)	TRL	Length of the whole root system
Total root surface area (cm^2)	TRSA	Surface area of the whole root system
Total root volume (cm^3)	TRV	Volume of the whole root system
Total primary root length (cm)	TPRL	Length of the whole primary root including axial root and lateral roots
Total primary root surface area (cm^2)	TPRSA	Surface area of the whole primary root
Total primary root volume (cm^3)	TPRV	Volume of the whole primary root
Primary root length (cm)	PRL	Measured with a ruler
Length of primary root apical unbranched zone (cm)	LAUZPR	Measured with a ruler
Length of visible lateral root zone (cm)	LVLRZ	PRL-LAUZPR; primary root length-length of primary root apical unbranched zone
Primary lateral root length (cm)	PLRL	TPRL-PRL; total primary root length-primary root length
Visible lateral root number of primary root	VLRNPR	Count of lateral roots from the first emerged lateral root on the primary root
Average lateral root length of primary root (cm)	ALRLPR	PLRL/VLRNPR; primary lateral root length/visible lateral root number of primary root
Visible lateral root density of primary root (cm^{-1})	VLRDPR	VLRNPR/LVLRZ; visible lateral root number of primary root/length of visible lateral root zone
Seminal root number	SRN	Count of the axial seminal roots
Seminal root length (cm)	SRL	Measured with a ruler
First whorl crown root number	FWCRN	Count of the axial first whorl crown roots
First whorl crown root length (cm)	FWCRL	Measured with a ruler
Average root diameter (mm)	ARD	Average diameter of the whole root system
Average primary root diameter (mm)	APRD	Average diameter of the whole primary root

(1|line) + (1|experiment) + (1|repeat%in%experiment) + (1|line × experiment). Phenotypic values were normalized using "bestNormalize" in the R software. The skewness and kurtosis of the phenotypic values were calculated. When the absolute value of skewness was less than 3 and the absolute value of kurtosis less than 10, the phenotypic values were considered to be approximately normally distributed. BLUP values for each trait were processed with SPSS Statistics 19.0 software (SPSS Inc., Chicago, IL, USA.) for descriptive statistical analysis (mean, range, coefficient of variation), correlation analysis and principal component analysis (PCA). The values were then visualized with Origin 2018 (OriginLab Inc., Northampton, MA, USA.) software packages. The response of each trait to LN was represented by the increase or decrease of LN relative to HN, calculated as (LN – HN)/HN × 100%. Analysis of variance was fitted using the PROC GLM program of SAS 9.2 (SAS Institute, Cary, NC, USA.). The broad-sense heritability of each trait was calculated as follows [41]:

$$H^2 = \frac{\sigma_g^2}{\sigma_g^2 + \frac{\sigma_{gl}^2}{n} + \frac{\sigma_e^2}{nr}} \quad (1)$$

where σ_g^2 is genetic variance, σ_{gl}^2 is variance of interaction between genotype and environment, σ_e^2 is error variance, n is the number of independent experiments, and r is the number of replicates.

2.5. Genome-wide association mapping

Trait associations were evaluated using TASSEL 5.0 software [42]. To reduce false negatives and false positives in the identification of significant SNP associations, a mixed linear model (MLM), which simultaneously controls population structure (Q) and kinship (K), as well as a general linear model (GLM), which controls only population structure (Q), were used to perform genome-wide association analysis between SNP markers and the 24 maize traits. A total of 542,796 high-quality SNP markers with a minimum allele frequency (MAF) greater than 0.05 were selected. The significance threshold of the marker was corrected by Bonferroni $P = \alpha/n$. At $\alpha = 1$ (MLM) and $\alpha = 0.05$ (GLM) levels, P-values were 1.84×10^{-6} (MLM) and 9.21×10^{-8} (GLM) and $-\log_{10}(P)$ values were 5.73 (MLM) and 7.04 (GLM) Further visualization of the data was performed using "CMplot" in the R software.

2.6. Haplotype and linkage disequilibrium (LD) block analysis

Allele effects of the most significant SNPs for candidate genes *GRMZM2G364901*, *GRMZM2G144744*, *GRMZM2G045070*, and *GRMZM2G159032* and corresponding phenotypic values were used for haplotype analysis. The data were then visualized with GraphPad Prism 7 software (GraphPad Software Inc., San Diego, CA, USA). LD-block analysis of these candidate genes was performed. Further visualization was performed using "LD heatmap" in the R software.

2.7. Annotation of candidate genes

Previous study [43] has shown that the LD distance of this population is 50 kb. Accordingly, using the B73 reference genome (RefGen-V2) in MaizeGDB (http://www.maizegdb.org/), the 50-kb range upstream and downstream of each significantly associated SNP locus was searched for candidate genes. Functional annotations of these genes were retrieved using the MaizeGDB Genome Browser [44]. The most likely candidate genes were selected based on the functional annotation of all genes near each locus and their expression in each tissue of B73 (MaizeGDB).

3. Results

3.1. Phenotypic variation in shoot and root traits

There was abundant genetic variation for each trait in the association panel and all phenotypic values were approximately normally distributed (Fig. 1). Under LN and HN conditions, the coefficients of variation of the 24 traits ranged from 14.09 to 81.39 and 13.80 to 79.50, respectively (Table S2). The fold changes in the 24 traits under LN varied 2.2–79.7 times among the population, with the lowest occurring in SPAD, ARD, and APRD and the highest in TRV, PLRL, and VLRNPR. Under HN, the fold changes in the 24 traits varied 2.4–67.0 times, with PH, SPAD, and ARD the lowest, and TPRL, PLRL, and VLRNPR the highest. The fold changes in each trait were relatively similar between the two N treatments, except for RSR and TPRV (Table S2).

Under LN conditions, genotype CIMBL51 had the smallest TRL, TRSA, and TPRSA trait values and CIMBL47 had the largest. Under HN conditions, CIMBL67 had the smallest TRSA, TRV, and PRL trait

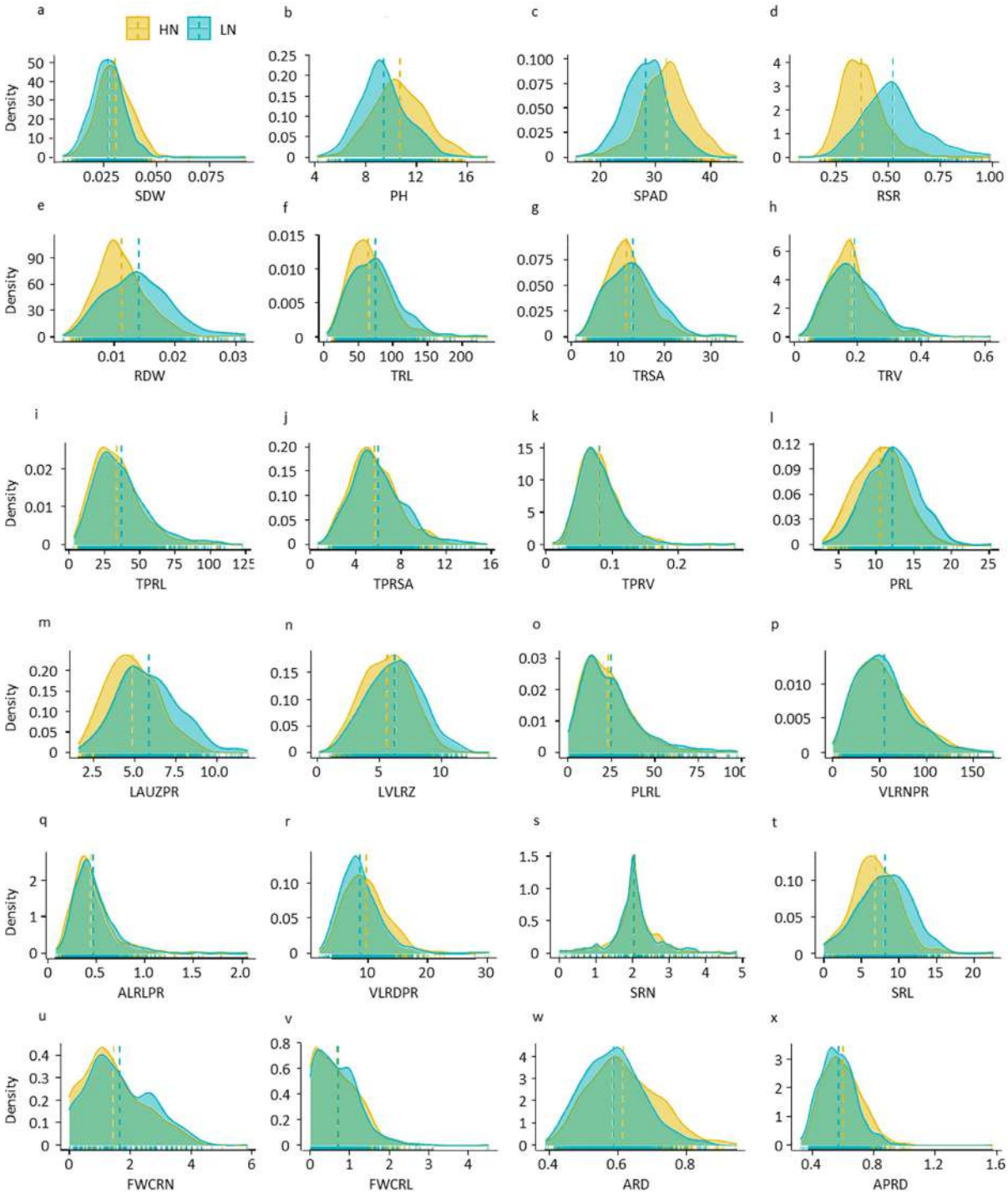

Fig. 1. Phenotypic distributions of the 24 investigated traits under high-N (HN) and low-N (LN) conditions. (a) Shoot dry weight. (b) Plant height. (c) SPAD value of the first leaf. (d) Root-to-shoot ratio. (e) Root dry weight. (f) Total root length. (g) Total root surface area. (h) Total root volume. (i) Total primary root length. (j) Total primary root surface area. (k) Total primary root volume. (l) Primary root length. (m) Length of the primary root apical unbranched zone. (n) Length of the visible lateral root zone. (o) Primary lateral root length. (p) Visible lateral root number of primary roots. (q) Average lateral root length of primary root. (r) Visible lateral root density of the primary root. (s) Seminal root number. (t) Seminal root length. (u) First whorl crown root number. (v) First whorl crown root length. (w) Average root diameter. (x) Average primary root diameter. The vertical yellow and blue broken lines represent the mean values of the population under HN and LN, respectively.

values and CIMBL65 had the largest. Among the traits, TRL, TRSA, TPRSA, TRV, and PRL were highly correlated (almost all $r > 0.50$, $P < 0.05$) (Fig. S1; Table S3).

3.2. Effect of low N on shoot and root growth

N treatment affected all of the plant traits except TPRV, VLRNPR, ALRLPR, SRN, and FWCRL. On average in the population, the LN treatment increased RSR by 40.4%, RDW by 26.1%, TRL by 15.8%, PRL by 15.4% and PLRL by 7.4%. LN treatment reduced SDW by 10.6%, PH by 12.2%, SPAD by 11.7%, VLRDPR by 11.1%, ARD by 4.8% and APRD by 5.2% (Fig. 2; Table S2). PCA clustered the traits into three groups: low-N increased, low-N reduced, and showing no response to low N. Within each group, there were high correlations between the traits (Figs. S1 and S2). The correlation coefficient between TRL and RDW was 0.67 under HN treatment and

0.75 after LN treatment. The correlation coefficients between TRL and TPRL and between PRL and PLRL were high at both N levels (r = 0.70 to 0.85). The correlations among TRL, SRN, and FWCRN were relatively low. There were significant positive correlations between ARD and APRD under both N treatments (r = 0.90). These two traits were negatively correlated with most of the other traits under both N treatments (Figs. S1 and S2; Table S3).

3.3. Genotype by environment effects on root growth

Under both N treatments, in comparison with the lines from the mixed, NSS, and TST subpopulations, the traits PH, SPAD, TRL, TPRL, LVLRZ, PLRL, VLRNPR, and VLRDPR were larger in the lines from the SS subpopulation (Fig. 3a–h). The mean value of traits LAUZPR, ARD, and APRD in the SS subpopulation was significantly smaller than those in the other subpopulations (Fig. 3i–k). The mean value of TPRSA was significantly higher in the SS subpopulation than in the other three subpopulations under LN but not HN (Fig. 3l). Low N treatment greatly increased the mean value of VLRNPR but did not affect that of VLRDPR in the SS lines (Fig. 3g, h). No difference was found between the SS and other subpopulations in the mean value of remaining 12 traits (Fig. S3).

Under LN conditions, the heritabilities of the traits ranged from 0.43 to 0.82, with FWCRL the lowest and PH the highest. Under HN conditions, the heritabilities were consistently reduced, ranging from 0.27 to 0.55. VLRDPR showed the lowest and PH the highest heritability (Table S2).

3.4. Genome-wide association analysis of shoot and root traits

A total of 328 significant SNP sites (MLM, $P < 1/n = 1.84 \times 10^{-6}$; GLM, $P < 0.05/n = 9.21 \times 10^{-8}$, n = 542,796) were identified. Under the LN condition, 23 significant SNP loci were identified by MLM. These loci were associated with 12 phenotypic traits: two shoot and 10 root traits. GLM identified 98 significant SNP loci. These too were associated with 12 phenotypic traits: two shoot and 10 root traits. Under HN conditions, 39 significant SNP loci for one shoot trait and eleven root traits were detected by MLM. GLM identified 168 significant SNP loci associated with one shoot and 16 root traits (Table 2).

Significant SNPs detected by both MLM and GLM were selected as high-priority markers. Under LN, nine such SNPs was selected. They were associated with six traits: one each with SDW, PH, and LVLRZ and two each with TRSA, VLRDPR, and FWCRN. Under HN, 25 effective SNPs were selected. These were associated with nine traits: one each with PH, RSR, RDW, TRV, and SRN and six with ALRLPR, nine with FWCRN, two with ARD, and three with APRD (Table 2). PH and FWCRN were associated with significant SNPs under both LN and HN treatment, suggesting that these two traits are associated with loci adapted to growth across different N levels. The other 11 traits showed significant SNP associations in either LN or HN but not both, suggesting that these traits respond uniquely to N level.

The 34 SNPs identified by both MLM and GLM were mapped to chromosomes 1 through 8. Further examination showed that only 12 regions were independent. For the 34 significant loci of the 13 traits, the variance ranged from 5.2% to 8.8%, with a mean P-value of 6.4% for MLM, and from 5.9% to 8.3%, with a mean P-value of 7.1% for GLM (Table S4).

3.5. Tentative candidate genes for the identified SNPs

For these 34 SNP loci, 55 candidate genes were identified, with one to eight genes per trait (Table S4). Under LN, two significant SNP-trait associations were found for TRSA and within the gene model *GRMZM2G364901* on chromosome 2 (Fig. 4a; Fig. 5a). This gene encodes protoporphyrinogen IX oxidase 2 and shows no difference in expression in the root under low or high N (Fig. S4). For TRSA, the most significant SNP was S2_34701035 for TRSA. The mean TRSA for the T allele was 12.47 cm^2, significantly lower that of the C allele, 17.11 cm^2 (Fig. 5b).

One LVLRZ-associated SNP region ($P = 1.16 \times 10^{-6}$, R^2 = 5.62, MLM) was found containing *GRMZM2G144744*, which encodes a DELLA protein (Fig. 4b; Fig. 5c). This gene was expressed differently under LN and HN in roots (Fig. S4). The mean LVLRZ for the A allele was 5.89 cm, significantly shorter than that of the G allele, 7.24 cm (Fig. 5d).

Significant loci were found for FWCRN under both HN and LN treatments (Fig. 4c, d; Fig. 5e, g). In this region, *GRMZM2G045070* encodes an MA3 domain-containing protein. This gene is involved in translation regulated by target of rapamycin (TOR). For the most significant SNPs S2_36837716 and S2_36835568 for FWCRN, the mean FWCRN under LN for the C allele was 1.54, significantly lower than that of the T allele, 2.49 (Fig. 5f). Under HN, the mean FWCRN for the G allele was 1.34, significantly lower than that of the C allele, 2.35 (Fig. 5h).

Under HN conditions, a candidate gene *GRMZM2G159032* that controls PH ($P = 3.46 \times 10^{-7}$, R^2 = 6.23, MLM) was found. It encodes

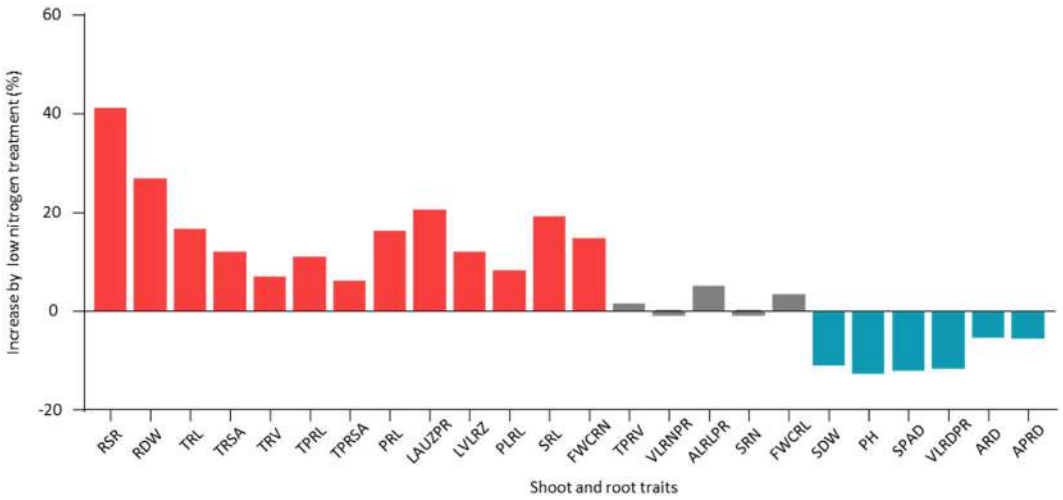

Fig. 2. Effect of low-N treatment on shoot and root growth. The values in red indicate traits that were increased by low N treatment. The values in blue indicate traits that were reduced by low-N treatment. The values in gray color indicate traits that were not affected by low-N treatment.

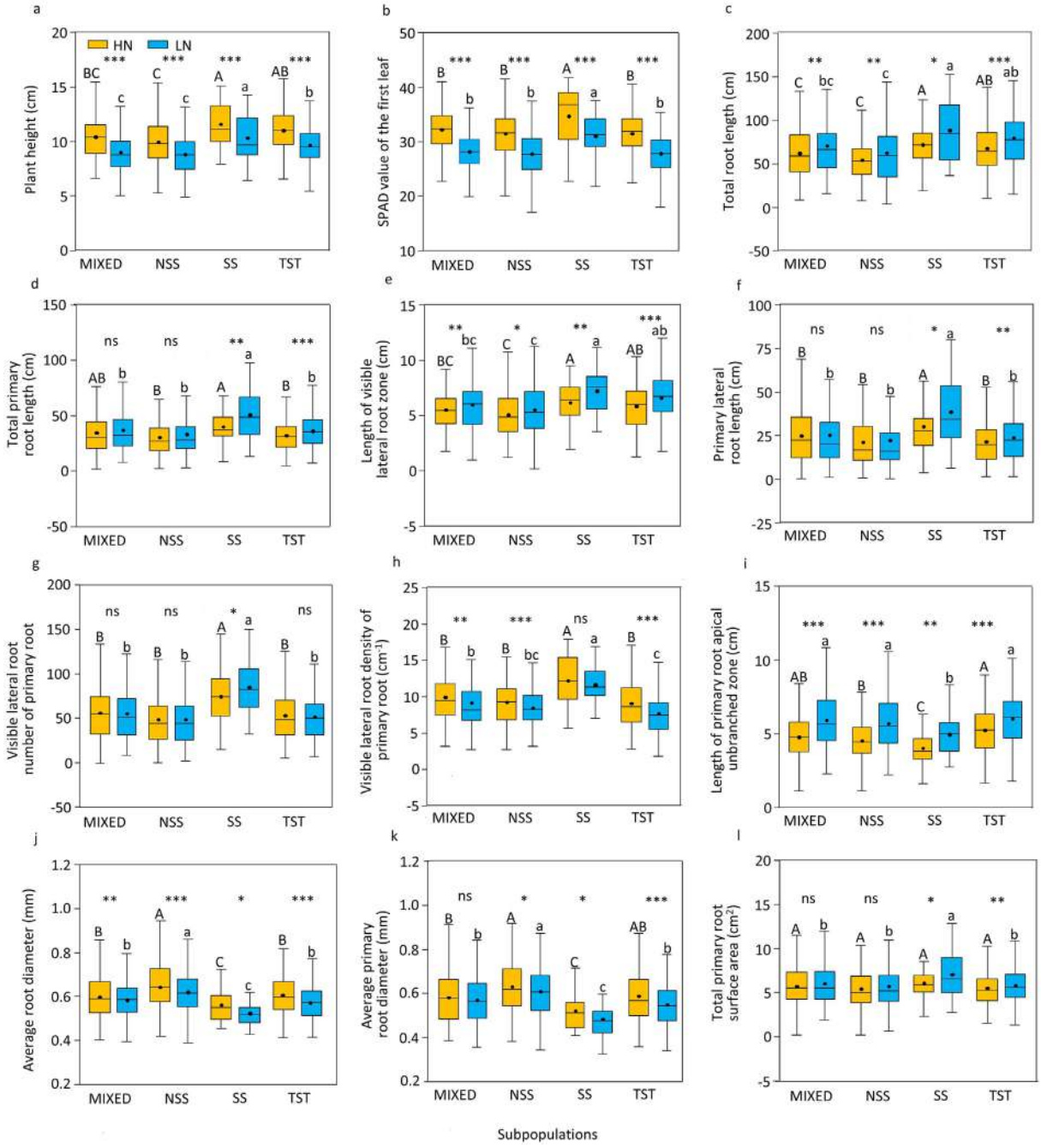

Fig. 3. Differential response of plant traits to N treatments among the four subpopulations. (a) Plant height. (b) SPAD value of the first leaf. (c) Total root length. (d) Total primary root length. (e) Length of the visible lateral root zone. (f) Primary lateral root length. (g) Visible lateral root number of primary roots. (h) Visible lateral root density of the primary root. (i) Length of the primary root apical unbranched zone. (j) Average root diameter. (k) Average primary root diameter. (l) Total primary root surface area. The solid line and black dot within each box represent the median and mean values, respectively. The top and bottom edge of each box represent the 75th and 25th percentiles, respectively. Significant differences between the four subpopulations at $P < 0.05$ are shown with different uppercase letters for HN and with lowercase letters for LN. *, **, and *** indicate significance at $P < 0.05$, $P < 0.01$, and $P < 0.001$ between HN and LN, respectively. ns, not significant.

histone deacetylase (Fig. 4e; Fig. 5i). The mean PH for the A allele was 11.93 cm, significantly lower than that of the T allele, 10.51 cm (Fig. 5j).

For the other eight traits, candidate genes were considered to be of lower priority (Fig. S5). Five SNPs linked to genes known to be involved in root development (Fig. S6; Table S5) were identified. The *rootless concerning crown and seminal roots* (*Rtcs*) gene [45] is located 240 kb from a SNP associated with TRV and ALRLPR. A significant SNP associated with SRN was slightly more than 1.2 Mb from the *root hair defective3* (*Rth3*) gene [46]. The SNP associated with FWCRL was located slightly more than 1.6 Mb from *Rtcs*. A SNP associated with LVLRZ in HN was located 1 Mb from *Rtcs-like1* (*Rtcl*) [45,47].

4. Discussion

4.1. Genotype by N interaction effect on early root growth

Many studies [18,19,22,30,31,48–50] have investigated maize root growth in response to low-N stress and its relationship with

Table 2
Number of significant SNPs detected for each trait.

Trait	LN			HN		
	MLM	GLM	JD	MLM	GLM	JD
SDW	1	1	1	0	0	0
PH	1	3	1	1	2	1
RSR	0	4	0	1	1	1
RDW	0	1	0	1	3	1
TRL	0	0	0	0	2	0
TRSA	4	2	2	0	8	0
TRV	0	8	0	1	21	1
TPRL	3	0	0	0	0	0
TPRSA	0	0	0	1	1	0
PRL	1	0	0	0	0	0
LVLRZ	1	1	1	0	2	0
PLRL	0	1	0	0	0	0
VLRNPR	0	0	0	1	3	0
ALRLPR	3	49	0	10	43	6
VLRDPR	2	4	2	0	3	0
SRN	2	0	0	1	1	1
SRL	1	2	0	0	8	0
FWCRN	2	22	2	9	25	9
FWCRL	2	0	0	2	6	0
ARD	0	0	0	7	22	2
APRD	0	0	0	4	17	3
Total	23	98	9	39	168	25

Numbers of SNPs are given as detected using MLM, GLM, or both (JD).

NUE. In previous studies [22,31,50], the endosperm was removed and root growth was evaluated at later seedling stages. To replicate true seedling growth conditions in this study, the endosperm was not removed, and root growth was evaluated at the germination stage. The finding that root growth responded to low N supply even at this early stage indicates that this method can be used for high-throughput phenotypic screens of maize germplasm.

In agreement with previous studies [22,31,50,51], plants grown under LN conditions showed reduced leaf chlorophyll content, PH, and shoot biomass, but increased root/shoot ratio compared to plants grown under HN conditions. This finding suggests that N-starved plants distribute more carbon to promote root growth in order to mine the substrate for more N. Root morphological traits were also shaped by low-N treatment. Longer TRL and larger TRSA indicate an increased ability to acquire N from soil profiles. At emergence, the primary root is the main component of the whole root system [14,52]. The correlation coefficients between TRL and TPRL and between PRL and PLRL were high, ranging from 0.70 to 0.85 (Fig. S1; Table S3), suggesting that primary root traits can be used as indicators of total root size. Low-N treatment also reduced ARD and APRD, but increased TRL and TPRL, indicating that under LN conditions, maize plants used less carbon to produce longer and thinner roots. This finding is consistent with those of Gao et al. [22] who showed that the root elongation rate was significantly increased under low-N stress and suggested that thinner roots under LN conditions are beneficial for reducing N consumption during root elongation. Similarly, Liu et al. [30] demonstrated low N-induced lateral root elongation in a recombinant inbred line population, and Li et al. [50] observed that low N increased lateral root length under LN conditions in a high-generation backcross population.

With respect to the genetic difference in root growth in response to low-N stress, the root/shoot ratio was increased in 426 lines and reduced in 35 lines, whereas RDW was increased in 373 lines and reduced in 88 lines. There were large genotypic differences for the other root traits, especially TPRV and VLRNPR. This finding indicates that there were strong genotype-by-N-environment interactions affecting root morphological traits. Indeed, compared with the lines from the mixed, NSS and TST subpopulations, the lines from the SS germplasm showed stronger ability to develop a large primary root system under LN conditions (Fig. 3). The SS germplasm may thus be a rich source of variation for low-N-tolerance breeding. Interestingly, Yang et al. [39] reported that SS showed the highest level of heterozygosity of SNPs among all the subpopulations.

Across the 24 traits, heritability under HN conditions was low to moderate (0.27–0.55), whereas heritability increased from moderate to high under LN conditions (0.43–0.82). Similar results were reported from other studies [31,38,50,51]. In our study, the h^2 of TRL, TPRL, PRL, and PLRL increased from 0.40–0.53 to 0.70–0.76 (Table S2), indicating that these root traits are more genetically controlled, and thus more amenable to genetic improvement under low-N environments.

4.2. GWAS and QTL analysis identify some common regions

Over the past few decades, numerous QTL affecting root phenotypes have been described in multiple maize populations [30,31,50,53–59]. Identification of consistent QTL in multiple mapping populations under multiple growth conditions is difficult but would be helpful for verifying our results and particularly to prioritize candidate genes underlying these traits.

Guo et al. [29] conducted a meta-analysis of 428 QTL associated with 23 maize root traits from 20 papers published between 2002 and 2018 and identified 53 meta-QTL over all the maize chromosomes. They also compared the meta-QTL with SNPs significantly associated with maize root traits reported from several GWAS projects [35,36,38]. Several meta-QTL were consistent with those found in our GWAS analysis. The 34 SNPs detected in our study were distributed on chromosomes 1 to 8, including six core regions in Bin 2.03, Bin 2.04, Bin 3.04, Bin 5.05, Bin 6.07, and Bin 8.05. These results show that GWAS is feasible for the study of root and shoot traits under different N treatments.

4.3. Complex molecular mechanisms of root and shoot growth under varying N conditions

By identifying five candidate genes in regions containing significant SNP markers, we investigated the possible molecular mechanisms affecting N-mediated root growth. Of course, these

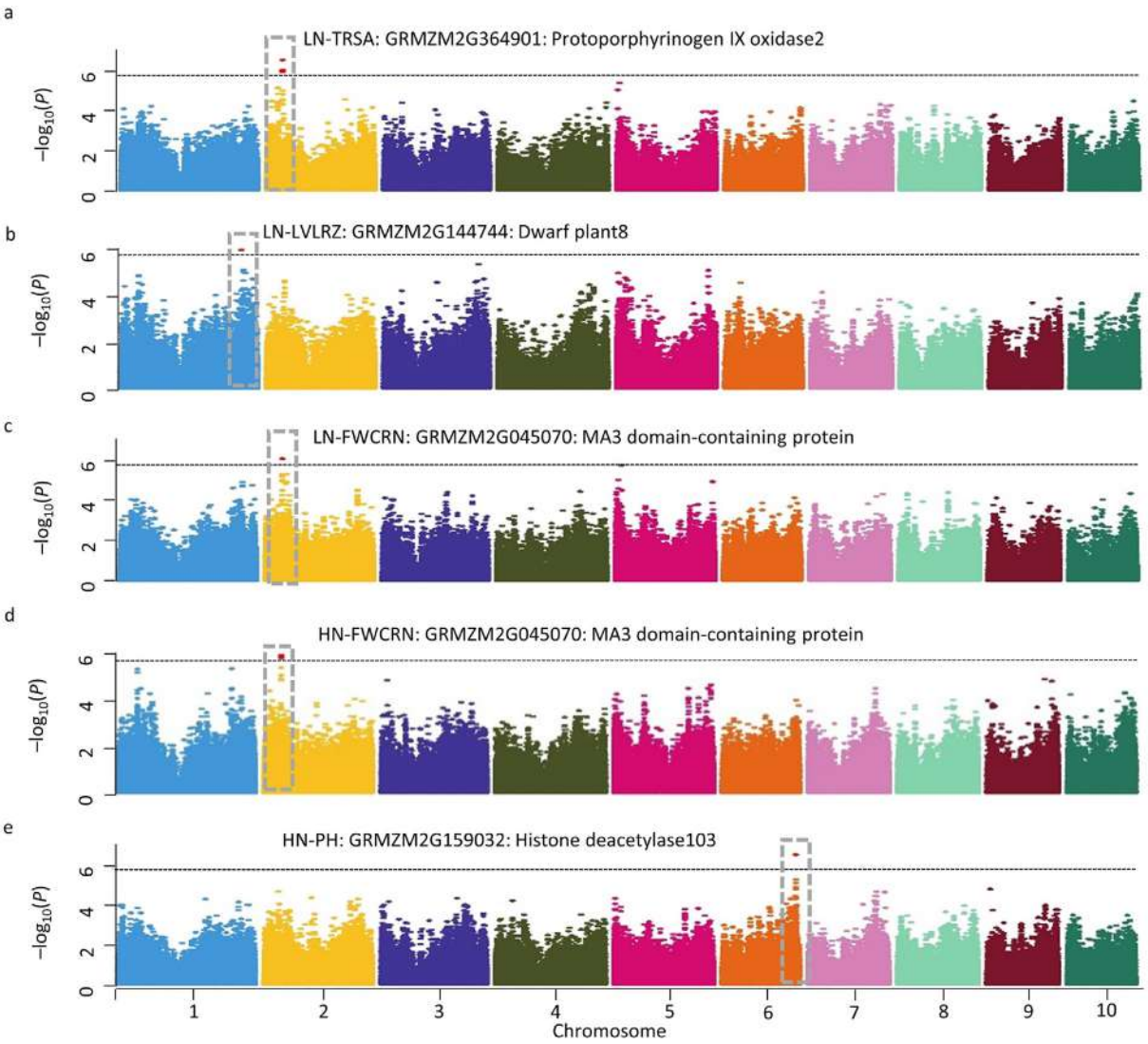

Fig. 4. Manhattan plots of TRSA (a), LVLRZ (b), and FWCRN (c) in LN and FWCRN (d) and PH (e) traits in HN using the mixed linear model (MLM). For each trait, the MLM mapping results are shown. The dotted horizontal gray line in the figure indicates the $-\log_{10}(P)$ significance threshold. Peaks with scores > $-\log_{10}(P)$ are outlined with dashed boxes and the corresponding potential candidate genes with annotations are indicated.

candidate genes have not been shown to be causative for the phenotypic variation observed in our GWAS panel. Furthermore, our methodology relied on identifying annotated genes within 100 kb of SNPs as located on the B73 genome [43]. For this reason, there may be loci more closely linked to our SNPs that were missed in our analysis. Nonetheless, it is interesting to speculate about gene functions that may account for the variation in traits. We checked the expression of *GRMZM2G364901*, *GRMZM2G144744*, *GRMZM2G159032*, and *GRMZM2G045070* in whole roots of B73 in response to N in previous studies [60–62] (Fig. S4). (1) Gene *GRMZM2G364901*, located in Bin 2.04, contained two SNPs that were significantly associated with TRSA under LN conditions. This gene is expressed in both maize shoots and roots [63]. In *Arabidopsis*, it encodes PPO2, a putative protoporphyrinogen oxidase known as MEE61 (maternal effect embryo arrest 61). Protoporphyrinogen is rapidly oxidized to protoporphyrin in the cytoplasm, producing large amounts of peroxide [64,65]. Zhao et al. [66] found that maize roots grown under LN conditions accumulated more H_2O_2 than those grown under HN conditions. Moreover, protoporphyrin can be processed to form heme, which induces root elongation [67]. Two studies [68,69] have shown that plant hemoglobin catalyzes the conversion of NO to nitrate. Trevisan et al. [70] found that the spatial distributions of nitrate reductase and hemoglobin transcripts in maize roots were regulated by nitrate. In roots, nitrate can act as a signal to induce its own sensing via nitrate reductase and hemoglobin dependent NO homeostasis. Nitrate sensing is involved in root elongation [71]. (2) The candidate gene *GRMZM2G144744*, located at Bin 1.09, contains a SNP associated with LVLRZ under LN. It is also known as dwarf plant 8 (*d8*) and encodes a DELLA protein. The *d8* gene and its three major dwarf alleles have previously been characterized at the molecular level. In *Arabidopsis*, auxin mediates root growth by increasing the degradation of gibberellin-responsive DELLA proteins [72]. It was also found [73] that ethylene can inhibit root elongation by stabilizing DELLA proteins. (3) *GRMZM2G159032*, located in Bin 6.07, contains one SNP marker that is associated with PH under HN. This gene encodes a histone deacetylase that is abundantly expressed in the stem and apical meristem [63,74,75]. Tian and Chen [76] reported that *athda19* mutants exhibit dwarfing, leaf malformation, and asymmetric leaf growth. In rice (*Oryza sativa* L.), down-regulation of OsHTD702 results in narrowed leaves and stems [77]. It is interesting to speculate that increased histone deacety-

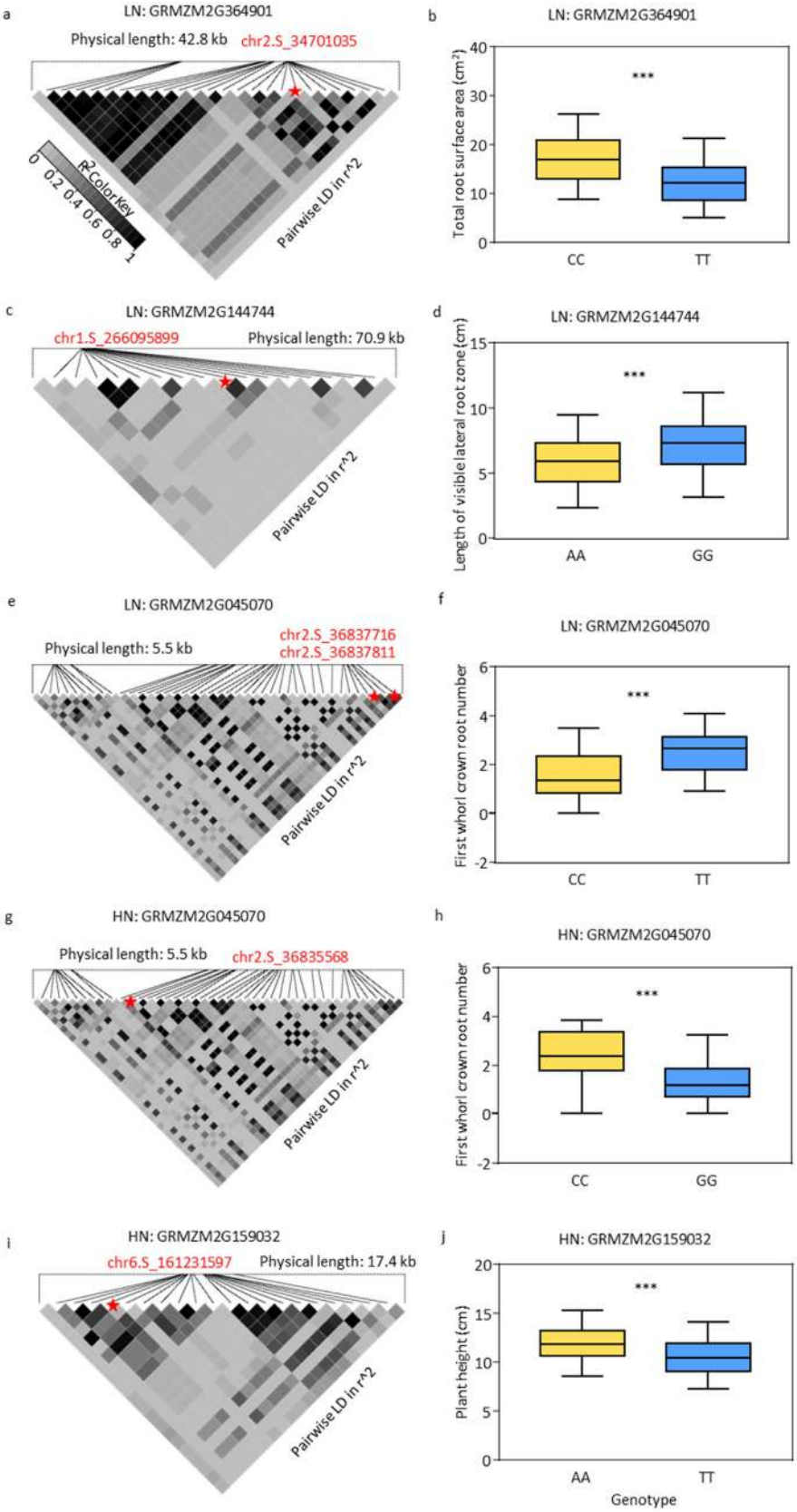

Fig. 5. LD patterns of SNPs in candidate genes and the allele effects of the most significant SNPs. (a and b) *GRMZM2G364901* LD pattern in LN and its most significant SNP allele effects. (c and d) *GRMZM2G144744* LD pattern in LN and its most significant SNP allele effects. (e and f) *GRMZM2G045070* LD pattern in LN and its most significant SNP allele effects. (g and h) *GRMZM2G045070* LD pattern in HN and its most significant SNP allele effects. (i and j) *GRMZM2G159032* LD pattern in HN and its most significant SNP allele effects. Red stars indicate the most significant SNP loci. For allele effects, the solid line in each box represents the median value. The top and bottom edges of each box represent the 75th and 25th percentiles, respectively. *** indicates significance at $P < 0.001$ of the difference between genotypes.

lase activity could increase growth and plant stature. (4) *GRMZM2G045070*, located in Bin 2.04, is associated with FWCRN under both LN and HN conditions. It encodes a MA3 domain-containing translation regulatory factor (MRF). The MRFs are thought [78] to interact with TOR to regulate protein synthesis, especially in response to nutrient and energy availability. In *Arabidopsis* roots, a TOR::GUS fusion protein is expressed in the quiescent center, apical meristem, and basal meristem. TOR kinase senses photosynthetic products, and signals and transports them from leaves to roots, thereby accelerating plant root elongation and root meristem division [79,80]. The TOR pathway regulates molecular and physiological adaptive responses to changes in N, glucose, and amino acid levels in cells [81,82].

CRediT authorship contribution statement

Xichao Sun: Writing - original draft. **Wei Ren:** Data curation. **Peng Wang:** Data curation. **Fanjun Chen:** Methodology. **Lixing Yuan:** Methodology. **Qingchun Pan:** Writing - review & editing. **Guohua Mi:** Writing - review & editing.

Declaration of competing interest

The authors declare that they have no known competing financial interests or personal relationships that could have appeared to influence the work reported in this paper.

Acknowledgments

This work was supported by the National Natural Science Foundation of China (31672221).

Appendix A. Supplementary data

Supplementary data for this article can be found online at https://doi.org/10.1016/j.cj.2020.09.011.

References

[1] H. Marschner, Mineral Nutrition of Higher Plants, Academic Press, London, UK, 1995.
[2] B. Hirel, J.L. Gouis, B. Ney, A. Gallais, The challenge of improving N use efficiency in crop plants: towards a more central role for genetic variability and quantitative genetics within integrated approaches, J. Exp. Bot. 58 (2007) 2369–2387.
[3] D. Tilman, K.G. Cassman, P.A. Matson, R. Naylor, S. Polasky, Agricultural sustainability and intensive production practices, Nature 418 (2002) 671.
[4] W.R. Raun, G.V. Johnson, Improving N use efficiency for cereal production, Agron. J. 91 (1999) 357.
[5] Z.L. Zhu, F.S. Zhang, Basic Research on N Behavior and Efficient Use of N Fertilizer in Main Farmland Ecosystems, Science Press, Beijing, China, 2010.
[6] D. Tilman, Global environmental impacts of agricultural expansion: the need for sustainable and efficient practices, Proc. Natl. Acad. Sci. U. S. A. 96 (1999) 5995–6000.
[7] J.M. Beman, K.R. Arrigo, P.A. Matson, Agricultural runoff fuels large phytoplankton blooms in vulnerable areas of the ocean, Nature 434 (2005) 211.
[8] J.H. Guo, X.J. Liu, Y. Zhang, J.L. Shen, W.X. Han, W.F. Zhang, P. Christie, K.W. Goulding, P.M. Vitousek, F.S. Zhang, Significant acidification in major Chinese croplands, Science 327 (2010) 1008–1010.
[9] X.T. Ju, G.X. Xing, X.P. Chen, S.L. Zhang, L.J. Zhang, X.J. Liu, Z.L. Cui, B. Yin, P. Christie, Z.L. Zhu, F.S. Zhang, Reducing environmental risk by improving N management in intensive Chinese agricultural systems, Proc. Natl. Acad. Sci. U. S. A. 106 (2009) 3041–3046.
[10] X.J. Liu, Y. Zhang, W.X. Han, A.H. Tang, J.L. Shen, Z.L. Cui, P.M. Vitousek, J.W. Erisman, K. Goulding, P. Christie, A. Fangmeier, F.S. Zhang, Enhanced N deposition over China, Nature 494 (2013) 459.
[11] FAOSTAT, FAO Statistical Databases, August 2000 ed, Food and agriculture organization of the United Nations, Rome, 2000.
[12] Y. Anbessa, P. Juskiw, A. Good, J. Nyachiro, J. Helm, Selection efficiency across environments in improvement of barley yield for moderately low N environments, Crop Sci. 50 (2010) 451–457.
[13] A.D. Mackay, S.A. Barber, Effect of N on root growth of two corn genotypes in the field, Agron. J. 78 (1986) 699–703.
[14] J.P. Lynch, Steep, cheap and deep: an ideotype to optimize water and N acquisition by maize root systems, Ann. Bot. 112 (2013) 347–357.
[15] S. Trachsel, S.M. Kaeppler, K.M. Brown, J.P. Lynch, Maize root growth angles become steeper under low N conditions, Field Crops Res. 140 (2013) 18–31.
[16] X.H. Mu, F.J. Chen, Q.P. Wu, Q.W. Chen, J.F. Wang, L.X. Yuan, G.H. Mi, Genetic improvement of root growth increases maize yield via enhanced post-silking N uptake, Eur. J. Agron. 63 (2015) 55–61.
[17] P. Yu, X.X. Li, P.J. White, C.J. Li, A large and deep root system underlies high N-use efficiency in maize production, PLoS ONE 10 (2015) e0126293.
[18] Q.Y. Tian, F.J. Chen, F.S. Zhang, G.H. Mi, Possible involvement of cytokinin in nitrate-mediated root growth in maize, Plant Soil 277 (2005) 185.
[19] Q.Y. Tian, F.J. Chen, J.X. Liu, F.S. Zhang, G.H. Mi, Inhibition of maize root growth by high nitrate supply is correlated with reduced IAA levels in roots, J. Plant Physiol. 165 (2008) 942–951.
[20] A.C.M. Gaudin, S.A. Mcclymont, B.M. Holmes, E. Lyons, M.N. Raizada, Novel temporal, fine-scale and growth variation phenotypes in roots of adult-stage maize (*Zea mays* L.) in response to low N stress, Plant Cell Environ. 34 (2011) 2122–2137.
[21] Y. Wang, G.H. Mi, F.J. Chen, J.H. Zhang, F.S. Zhang, Response of root morphology to nitrate supply and its contribution to N accumulation in maize, J. Plant Nutr. 27 (2005) 2189–2202.
[22] K. Gao, F.J. Chen, L.X. Yuan, G.H. Mi, A comprehensive analysis of root morphological changes and N allocation in maize in response to low N stress, Plant Cell Environ. 38 (2015) 740–750.
[23] F. Wiesler, W.J. Horst, Differences between maize cultivars in yield formation, N uptake and associated depletion of soil nitrate, J. Agron. Crop Sci. 168 (1992) 226–237.
[24] J. King, A. Gay, R. Sylvester-Bradley, I. Bingham, J. Foulkes, P. Gregory, D. Robinson, Modelling cereal root systems for water and N capture: towards an economic optimum, Ann. Bot. 91 (2003) 383–390.
[25] G.H. Mi, F.J. Chen, Q.P. Wu, N.W. Lai, L.X. Yuan, F.S. Zhang, Ideotype root architecture for efficient N acquisition by maize in intensive cropping systems, Sci. China Life Sci. 53 (2010) 1369–1373.
[26] G.H. Mi, F.J. Chen, L.X. Yuan, F.S. Zhang, Ideotype root system architecture for maize to achieve high yield and resource use efficiency in intensive cropping systems, Adv. Agron. 139 (2016) 73–97.
[27] A.L. Bray, C.N. Topp, The quantitative genetic control of root architecture in maize, Plant Cell Physiol. 59 (2018) 1919–1930.
[28] A. Hund, R. Reimer, R. Messmer, A consensus map of QTLs controlling the root length of maize, Plant Soil 344 (2011) 143–158.
[29] J. Guo, L. Chen, Y.X. Li, Y.S. Shi, Y.C. Song, D.F. Zhang, Y. Li, T.Y. Wang, D.G. Yang, C.H. Li, Meta-QTL analysis and identification of candidate genes related to root traits in maize, Euphytica 214 (2018) 223.
[30] J.C. Liu, J.S. Li, F.J. Chen, F.S. Zhang, T.H. Ren, Z.J. Zhuang, G.H. Mi, Mapping QTLs for root traits under different nitrate levels at the seedling stage in maize (*Zea mays* L), Plant Soil 305 (2008) 253–265.
[31] P.C. Li, F.J. Chen, H.G. Cai, J.C. Liu, Q.C. Pan, Z.G. Liu, R.L. Gu, G.H. Mi, F.S. Zhang, L.X. Yuan, A genetic relationship between N use efficiency and seedling root traits in maize as revealed by QTL analysis, J. Exp. Bot. 66 (2015) 3175–3188.
[32] E. Pestsova, D. Lichtblau, C. Wever, T. Presterl, T. Bolduan, M. Ouzunova, P. Westhoff, QTL mapping of seedling root traits associated with N and water use efficiency in maize, Euphytica 209 (2016) 585–602.
[33] C. Andorf, W.D. Beavis, M. Hufford, S. Smith, W.P. Suza, K. Wang, M. Woodhouse, J.M. Yu, T. Lübberstedt, Technological advances in maize breeding: past, present and future, Theor. Appl. Genet. 132 (2019) 817–849.
[34] J.M. Yu, E.S. Buckler, Genetic association mapping and genome organization of maize, Curr. Opin. Biotechnol. 17 (2006) 155–160.
[35] J. Pace, C. Gardner, C. Romay, B. Ganapathysubramanian, T. Lübberstedt, Genome-wide association analysis of seedling root development in maize (*Zea mays* L.), BMC Genomics 16 (2015) 47.
[36] P.H. Zaidi, K. Seetharam, G. Krishna, L. Krishnamurthy, S. Gajanan, R. Babu, M. Zerka, M.T. Vinayan, B.S. Vivek, Genomic regions associated with root traits under drought stress in tropical maize (*Zea mays* L.), PLoS ONE 11 (2016) e0164340.
[37] J.S. Morosini, L.D.F. Mendonça, D.H. Lyra, G. Galli, M.S. Vidotti, R. Fritsche-Neto, Association mapping for traits related to N use efficiency in tropical maize lines under field conditions, Plant Soil 421 (2017) 453–463.
[38] D.L. Sanchez, S.S. Liu, R. Ibrahim, M. Blanco, T. Lübberstedt, Genome-wide association studies of doubled haploid exotic introgression lines for root system architecture traits in maize (*Zea mays* L.), Plant Sci. 268 (2018) 30–38.
[39] X.H. Yang, S.B. Gao, S.T. Xu, Z.X. Zhang, B.M. Prasanna, L. Li, J.S. Li, J.B. Yan, Characterization of a global germplasm collection and its potential utilization for analysis of complex quantitative traits in maize, Mol. Breed. 28 (2011) 511–526.
[40] F. Hochholdinger, R. Tuberosa, Genetic and genomic dissection of maize root development and architecture, Curr. Opin. Plant Biol. 12 (2009) 172–177.
[41] S.J. Knapp, W.W. Stroup, W.M. Ross, Exact confidence intervals for heritability on a progeny mean basis 1, Crop Sci. 25 (1985) 192–194.
[42] P.J. Bradbury, Z.W. Zhang, D.E. Kroon, T.M. Casstevens, Y. Ramdoss, E.S. Buckler, TASSEL: software for association mapping of complex traits in diverse samples, Bioinformatics 23 (2007) 2633–2635.
[43] H. Li, Z.Y. Peng, X.H. Yang, W.D. Wang, J.J. Fu, J.H. Wang, Y.J. Han, Y.C. Chai, T.T. Guo, N. Yang, J. Liu, M.L. Warburton, Y.B. Cheng, X.M. Hao, P. Zhang, J.Y. Zhao, Y.J. Liu, G.Y. Wang, J.S. Li, J.B. Yan, Genome-wide association study dissects the genetic architecture of oil biosynthesis in maize kernels, Nat. Genet. 45 (2013) 43.

[44] C.M. Andorf, C.J. Lawrence, L.C. Harper, M.L. Schaeffer, D.A. Campbell, T.Z. Sen, The Locus Lookup tool at MaizeGDB: identification of genomic regions in maize by integrating sequence information with physical and genetic maps, Bioinformatics 26 (2010) 434–436.
[45] G. Taramino, M. Sauer, J.L. Stauffer, D. Multani, X.M. Niu, H. Sakai, F. Hochholdinger, The maize (*Zea mays* L.) *RTCS* gene encodes a LOB domain protein that is a key regulator of embryonic seminal and post-embryonic shoot-borne root initiation, Plant J. 50 (2007) 649–659.
[46] F. Hochholdinger, T.J. Wen, R. Zimmermann, P. Chimot-Marolle, O. da Costa, W. e Silva Bruce, K.R. Lamkey, U. Wienand, P.S. Schnable, The maize (*Zea mays* L.) *roothairless3* gene encodes a putative GPI-anchored, monocot-specific, COBRA-like protein that significantly affects grain yield, Plant J. 54 (2008) 888–898.
[47] C.Z. Xu, H.H. Tai, M. Saleem, Y. Ludwig, C. Majer, K.W. Berendzen, K.A. Nagel, T. Wojciechowski, R.B. Meeley, G. Taramino, F. Hochholdinger, Cooperative action of the paralogous maize lateral organ boundaries (LOB) domain proteins RTCS and RTCL in shoot-borne root formation, New Phytol. 207 (2015) 1123–1133.
[48] L. Chun, G.H. Mi, J.S. Li, F.J. Chen, F.S. Zhang, Genetic analysis of maize root characteristics in response to low N stress, Plant Soil 276 (2005) 369–382.
[49] A.H. Abdel-Ghani, B. Kumar, J. Reyes-Matamoros, P.J. Gonzalez-Portilla, C. Jansen, J.P.S. Martin, M. Lee, T. Lübberstedt, Genotypic variation and relationships between seedling and adult plant traits in maize (*Zea mays* L.) inbred lines grown under contrasting N levels, Euphytica 189 (2013) 123–133.
[50] P.C. Li, Z.J. Zhuang, H.G. Cai, S. Cheng, A.A. Soomro, Z.G. Liu, R.L. Gu, G.H. Mi, L.X. Yuan, F.J. Chen, Use of genotype-environment interactions to elucidate the pattern of maize root plasticity to N deficiency, J. Integr. Plant Biol. 58 (2016) 242–253.
[51] L.G. Torres, D.G. Caixeta, W.M. Rezende, A. Schuster, C.F. Azevedo, F.F.E. Silva, R.O. DeLima, Genotypic variation and relationships among traits for root morphology in a panel of tropical maize inbred lines under contrasting N levels, Euphytica 215 (2019) 51.
[52] J.P. Lynch, Root architecture and plant productivity, Plant Physiol. 109 (1995) 7.
[53] R. Tuberosa, M.C. Sanguineti, P. Landi, M.M. Giuliani, S. Salvi, S. Conti, Identification of QTLs for root characteristics in maize grown in hydroponics and analysis of their overlap with QTLs for grain yield in the field at two water regimes, Plant Mol. Biol. 48 (2002) 697–712.
[54] A. Hund, Y. Fracheboud, A. Soldati, E. Frascaroli, S. Salvi, P. Stamp, QTL controlling root and shoot traits of maize seedlings under cold stress, Theor. Appl. Genet. 109 (2004) 618–629.
[55] J.M. Zhu, S.M. Kaeppler, J.P. Lynch, Mapping of QTLs for lateral root branching and length in maize (*Zea mays* L.) under differential phosphorus supply, Theor. Appl. Genet. 111 (2005) 688–695.
[56] J.M. Zhu, S.M. Mickelson, S.M. Kaeppler, J.P. Lynch, Detection of quantitative trait loci for seminal root traits in maize (*Zea mays* L.) seedlings grown under differential phosphorus levels, Theor. Appl. Genet. 113 (2006) 1–10.
[57] H.G. Cai, F.J. Chen, G.H. Mi, F.S. Zhang, H.P. Maurer, W.X. Liu, J.C. Reif, L.X. Yuan, Mapping QTLs for root system architecture of maize (*Zea mays* L.) in the field at different developmental stages, Theor. Appl. Genet. 125 (2012) 1313–1324.
[58] W.B. Song, B.B. Wang, A.L. Hauck, X.M. Dong, J.P. Li, J.S. Lai, Genetic dissection of maize seedling root system architecture traits using an ultra-high density bin-map and a recombinant inbred line population, J. Integr. Plant Biol. 58 (2016) 266–279.
[59] Z.G. Liu, K. Gao, S.C. Shan, R.L. Gu, Z.K. Wang, E.J. Craft, G.H. Mi, L.X. Yuan, F.J. Chen, Comparative analysis of root traits and the associated QTLs for maize seedlings grown in paper roll, hydroponics and vermiculite culture system, Front. Plant Sci. 8 (2017) 436.
[60] S. Mager, U. Ludewig, Massive loss of DNA methylation in N-, but not in phosphorus-deficient *Zea mays* roots is poorly correlated with gene expression differences, Front. Plant Sci. 9 (2018) 497.
[61] Y.C. Wang, J.Y. Xu, M. Ge, L.H. Ning, M.M. Hu, H. Zhao, High-resolution profile of transcriptomes reveals a role of alternative splicing for modulating response to N in maize, BMC Genomics 21 (2020) 353.
[62] X.J. He, H.X. Ma, X.W. Zhao, S.J. Nie, Y.H. Li, Z.M. Zhang, Y. Shen, Q. Chen, Y.L. Lu, H. Lan, S.F. Zhou, S.B. Gao, G.T. Pan, H.J. Lin, Comparative RNA-Seq analysis reveals that regulatory network of maize root development controls the expression of genes in response to N stress, PLoS ONE 11 (2016) e0151697.
[63] R.S. Sekhon, H.N. Lin, K.L. Childs, C.N. Hansey, C.R. Buell, N.D. Leon, S.M. Kaeppler, Genome-wide atlas of transcription during maize development, Plant J. 66 (2011) 553–563.
[64] J.M. Jacobs, N.J. Jacobs, Porphyrin accumulation and export by isolated barley (*Hordeum vulgare*) plastids (effect of diphenyl ether herbicides), Plant Physiol. 101 (1993) 1181–1187.
[65] H.J. Lee, M.V. Duke, S.O. Duke, Cellular localization of protoporphyrinogen-oxidizing activities of etiolated barley (*Hordeum vulgare* L.) leaves (relationship to mechanism of action of protoporphyrinogen oxidase-inhibiting herbicides), Plant Physiol. 102 (1993) 881–889.
[66] D.Y. Zhao, Q.Y. Tian, L.H. Li, W.H. Zhang, Nitric oxide is involved in nitrate-induced inhibition of root elongation in *Zea mays*, Ann. Bot. 100 (2007) 497–503.
[67] W. Xuan, L.Q. Huang, M. Li, B.K. Huang, S. Xu, H. Liu, Y. Gao, W.B. Shen, Induction of growth elongation in wheat root segments by heme molecules: a regulatory role of carbon monoxide in plants?, Plant Growth Regul. 52 (2007) 41–51.
[68] M. Perazzolli, P. Dominici, M.C. Romero-Puertas, E. Zago, J. Zeier, M. Sonoda, C. Lamb, M. Delledonne, *Arabidopsis* nonsymbiotic hemoglobin AHb1 modulates nitric oxide bioactivity, Plant Cell 16 (2004) 2785–2794.
[69] K.H. Hebelstrup, M.V. Zanten, J. Mandon, L.A.C.J. Voesenek, F.J.M. Harren, S.M. Cristescu, I.M. Møller, L.A.J. Mur, Haemoglobin modulates NO emission and hyponasty under hypoxia-related stress in *Arabidopsis thaliana*, J. Exp. Bot. 63 (2012) 5581–5591.
[70] S. Trevisan, A. Manoli, M. Begheldo, A. Nonis, M. Enna, S. Vaccaro, G. Caporale, B. Ruperti, S. Quaggiotti, Transcriptome analysis reveals coordinated spatiotemporal regulation of hemoglobin and nitrate reductase in response to nitrate in maize roots, New Phytol. 192 (2011) 338–352.
[71] A. Manoli, M. Begheldo, A. Genre, L. Lanfranco, S. Trevisan, S. Quaggiotti, NO homeostasis is a key regulator of early nitrate perception and root elongation in maize, J. Exp. Bot. 65 (2013) 185–200.
[72] X.D. Fu, N.P. Harberd, Auxin promotes *Arabidopsis* root growth by modulating gibberellin response, Nature 421 (2003) 740.
[73] P. Achard, W.H. Vriezen, D.V.D. Straeten, N.P. Harberd, Ethylene regulates *Arabidopsis* development via the modulation of DELLA protein growth repressor function, Plant Cell 15 (2003) 2816–2825.
[74] A. Lusser, G. Brosch, A. Loidl, H. Haas, P. Loidl, Identification of maize histone deacetylase HD2 as an acidic nucleolar phosphoprotein, Science 277 (1997) 88–91.
[75] K.Q. Wu, L.N. Tian, K. Malik, D. Brown, B. Miki, Functional analysis of HD2 histone deacetylase homologues in *Arabidopsis thaliana*, Plant J. 22 (2000) 19–27.
[76] L. Tian, Z.J. Chen, Blocking histone deacetylation in *Arabidopsis* induces pleiotropic effects on plant gene regulation and development, Proc. Natl. Acad. Sci. U. S. A. 98 (2001) 200–205.
[77] Y.F. Hu, F.J. Qin, L.M. Huang, Q.W. Sun, C. Li, Y. Zhao, D.X. Zhou, Rice histone deacetylase genes display specific expression patterns and developmental functions, Biochem. Biophys. Res. Commun. 388 (2009) 266–271.
[78] D.H. Lee, S.J. Park, C.S. Ahn, H.S. Pai, MRF family genes are involved in translation control, especially under energy-deficient conditions, and their expression and functions are modulated by the TOR signaling pathway, Plant Cell 29 (2017) 2895–2920.
[79] Y. Xiong, J. Sheen, Rapamycin and glucose-target of rapamycin (TOR) protein signaling in plants, J. Biol. Chem. 287 (2012) 2836–2842.
[80] Y. Xiong, J. Sheen, Moving beyond translation: glucose-TOR signaling in the transcriptional control of cell cycle, Cell Cycle 12 (2013) 1989–1990.
[81] M. Orlova, E. Kanter, D. Krakovich, S. Kuchin, N availability and TOR regulate the Snf1 protein kinase in saccharomyces cerevisiae, Eukaryot. Cell 5 (2006) 1831–1837.
[82] K.A. Staschke, S. Dey, J.M. Zaborske, L.R. Palam, J.N. McClintick, T. Pan, H.J. Edenberg, R.C. Wek, Integration of general amino acid control and target of rapamycin (TOR) regulatory pathways in N assimilation in yeast, J. Biol. Chem. 285 (2010) 16893–16911.